PHYSICAL REVIEW B **81**, 081104(R) (2010)

Reorientable dipolar Cu_{Ca} antisite and anomalous screening in $CaCu_3Ti_4O_{12}$

Pietro Delugas,[1,2] Paola Alippi,[3] Vincenzo Fiorentini,[2] and Vito Raineri[1]

[1]*CNR-IMM, Istituto per la Microelettronica e Microsistemi, Consiglio Nazionale delle Ricerche, Stradale Primosole 50, 95121 Catania, Italy*

[2]*CNR-IOM-SLACS, Istituto Officina dei Materiali, Consiglio Nazionale delle Ricerche, and Dipartimento di Fisica, Università di Cagliari, Cittadella Universitaria, Monserrato, 09042 Cagliari, Italy*

[3]*CNR-ISM, Istituto di Struttura della Materia, Consiglio Nazionale delle Ricerche, Via Salaria km 29.5, CP 10, 00016 Monterotondo Stazione, Italy*

(Received 2 November 2009; revised manuscript received 31 December 2009; published 24 February 2010)

Based on first-principles calculations, we show that the abundant Cu_{Ca} antisite defect contributes sizably to dielectric screening in single-crystal $CaCu_3Ti_4O_{12}$. Cu_{Ca} has a multi-minimum off-center equilibrium configuration, whereby it possesses a large and easily reorientable dipole moment. The low-temperature and frequency cut-off behavior of Cu_{Ca}-induced response is consistent with experiment.

DOI: 10.1103/PhysRevB.81.081104 PACS number(s): 61.72.Bb, 71.15.Mb, 77.22.Ch

The multiple-perovskite $CaCu_3Ti_4O_{12}$ (CCTO) has stimulated intense interest due to the peculiar behavior[1] of its dielectric constant, which reaches values as high as $\sim 10^5$, is almost temperature insensitive from 100 to 500 K, and is cut off down to less than 10^2 at frequencies around 10 MHz. A prominent explanation[2–5] is that the giant permittivity is nonintrinsic and due to space charge at material inhomogeneities. Polycrystalline phases appear to exhibit insulating boundaries[6,7] between conducting grains, whose overall behavior is compatible with that of so-called internal barrier layer capacitors. (Incidentally, both the origin of intrinsic conductivity and the nature of electrical discontinuities are still debated.) This interpretation, however, does not apply to single crystals: it is plausible that the study of lattice defects therein will offer useful clues.

In this Rapid Communication we study *A*-site antisite defects via first-principles calculations and identify the Cu_{Ca} antisite as an interesting candidate for anomalous dielectric response: it has a multi-minimum equilibrium configuration with large dipole moment; it is easily reoriented; it can exist in large concentrations; and a simple analysis suggests that its contribution to screening will be exceptionally strong and with a temperature and frequency behavior consistent with experiments. Also, it is an abundant defect in typically accessible conditions.

CCTO owes many of its properties to the specific pattern of *A*-site occupation. Both its magnetic structure (G-type antiferromagnet, $T_N=29$ K) and Mott insulator nature (with a transport gap of ~ 0.7 eV between prevailingly Cu *d*-like states, according to our calculations[8] and recent experiments[9]) stem from the presence of plaquette-coordinated Cu^{2+} ions. The ionic dielectric response[10] of the lattice is in turn dominated by soft mostly Ca-localized vibrations. A strong randomization of *A*-site occupations is unlikely because Ca and Cu sites are not interchangeable: out of four *A* sites in the primitive cell, only the Ca site is a canonical perovskitic cubic site; the other three *A* sites host Cu—a strong Jahn-Teller ion in the 2+ state—which binds to four octahedron-vertex oxygens and forms thereby a planar CuO_4 complex, thanks to the coordinated tilting of TiO_6 octahedra. The three CuO_4 plaquettes per unit cell are mutually orthogonal, thus preserving the overall cubic symmetry. Cationic disorder in CCTO, therefore, will occur as a small perturbation of the ordered arrangement and can be addressed in terms of independent antisites.

We assess the properties of anti-site defects by first-principles methods. Relaxed structures, formation energies, and related observables are obtained by gradient-corrected (GGA)[11] density-functional theory (PW91 functional), and specifically with the VASP (Ref. 12) implementation of the all-electron projector augmented wave (PAW) method.[13] A cut-off energy of 400 eV was adopted for the plane-wave basis. We use throughout[14] the theoretical lattice parameter $a_0=7.41$ Å (+0.5% from experiment). Bulk calculations are performed in a simple cubic[15] 40 atom cell, which includes two formula units as needed for magnetic calculations. Defect calculations used an 80 atom, $a=2a_0$, face-centered-cubic supercell. The Brillouin-zone integration uses $4\times4\times4$ and $2\times2\times2$ grids for the bulk and defected cell, respectively. Charge-state corrections[16] are included when applicable. The predicted bulk electronic structure is, as observed, antiferromagnetic and insulating. The two latter characters are essentially preserved in the defected system. Structural optimizations were performed until all force components were below 0.01 eV/Å. Defect concentrations are calculated (neglecting vibrational formation entropy) as

$$N_{\mathrm{def}}(\mathrm{T}) = N_C \exp(-E_{\mathrm{form}}/k_B\mathrm{T}), \tag{1}$$

where N_C is the density of potentially defected sites (1.5 and 0.5×10^{22} cm^{-3} for Ca_{Cu} and Cu_{Ca}, respectively) and T is the growth temperature. The formation energy E_{form} is obtained as usual from total energies as

$$E_{\mathrm{form}} = E_{\mathrm{def}} - E_{\mathrm{bulk}} - \sum_{\nu} \Delta_\nu \mu_\nu. \tag{2}$$

The total energies E_{def} and E_{bulk} of the defected and bulk supercell, respectively, are not directly comparable as the cells generally contain different numbers of ions of each species. This is accounted for by the chemical potentials μ_ν of each species ν, and the differences Δ_ν between the number of atoms of a given species in the defected and bulk supercells. In our case, the cells differ only by having one Cu more and one Ca less for Cu_{Ca}, and vice versa for Ca_{Cu}. Thus, the

 ©2010 The American Physical Society

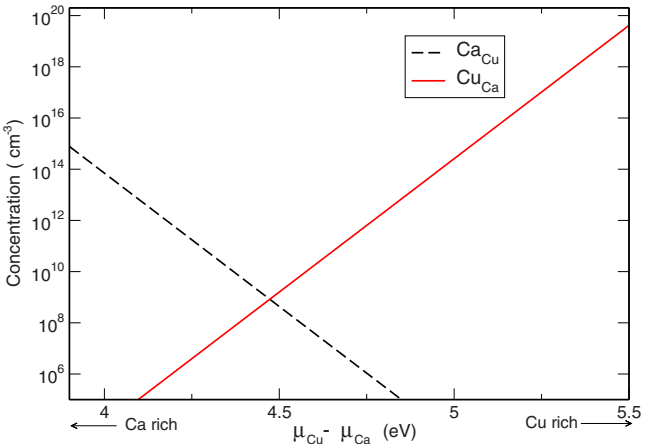

FIG. 1. (Color online) Cationic antisite concentrations from Ca-rich to Cu-rich conditions at T=500 K. The range of the chemical potential difference is the enthalpy of formation of CuO.

formation energies of Cu_{Ca} and Ca_{Cu}, and hence their concentrations, depend on the difference of Ca and Cu chemical potentials, $\mu_{Cu}-\mu_{Ca}$. Concentrations at $T=500$ K are sketched in Fig. 1 as functions of $\mu_{Cu}-\mu_{Ca}$ (see the discussion below).

Thermodynamic equilibrium conditions should be imposed on the chemical potentials. Equilibrium with CCTO imposes

$$\mu_{Ca}+3\mu_{Cu}+4\mu_{Ti}+12\mu_{O}=E_{bulk}^{CCTO}, \tag{3}$$

with E_{bulk}^{CCTO} the energy of CCTO per formula unit. Next, since $CaTiO_3$ precipitation in the form of inclusions is expected and reported[17] to occur in CCTO,

$$\mu_{Ca}+\mu_{Ti}+3\mu_{O}=E_{bulk}^{CaTiO_3}, \tag{4}$$

with $E_{bulk}^{CaTiO_3}$ is the energy of $CaTiO_3$ per formula unit.

Combining Eqs. (3) and (4) into

$$[\mu_{Cu}-\mu_{Ca}]_{Ca-rich}=(E_{bulk}^{CCTO}-4E_{bulk}^{CaTiO_3})/3, \tag{5}$$

we describe equilibrium with CCTO and $CaTiO_3$. This corresponds to Ca-rich conditions, i.e., to $\mu_{Cu}-\mu_{Ca}$ at the left end of Fig. 1. The formation energies are 0.7 eV for Ca_{Cu} and 1.8 eV for Cu_{Ca}, i.e., the former is favored as expected in Ca-rich conditions. Chemical potential differences off the left end of Fig. 1 represent $CaTiO_3$ precipitation conditions. The highest possible Ca_{Cu} concentration is therefore a modest 7×10^{14} cm^{-3} at 500 K.

Now, experiments also suggest that Cu excess off-stoichiometries will result in CuO precipitation. This may be described by the further constraint

$$\mu_{Cu}+\mu_{O}=E_{bulk}^{CuO} \tag{6}$$

on Cu and O chemical potentials. While we may combine Eqs. (3), (4), and (6) to constrain all chemical potentials except one (e.g., that of oxygen), we can take a shorter route noting that the difference of μ_{Cu} between Cu-rich (O-lean) and Cu-lean (O-rich) conditions is the CuO formation enthalpy $\Delta H(CuO)\simeq-1.6$ eV/formula. The upper limit for Cu_{Ca} concentration is reached in extreme Cu rich conditions, with $\mu_{Cu}-\mu_{Ca}$ increased by $|\Delta H(CuO)|$. These conditions are met at the right end of Fig. 1: the Cu_{Ca} formation energy drops to 0.2 eV, yielding an upper-limit concentration of $N_{Cu_{Ca}}=4\times10^{19}$ cm^{-3} at 500 K. Therefore, Cu excess produces quite large amounts of Cu_{Ca} antisites, while Ca excess causes modest amounts of Ca_{Cu} antisites. We note that the oxygen vacancy may compete with Cu_{Ca} in the present O-lean growth conditions. However, we find that it can be safely neglected. Its formation energy in the neutral state is 0.9 eV and in the 2+ charge state it is 0.6 eV (lowest value, for Fermi level at valence-band top), and hence its calculated concentration at 500 K is three to six orders of magnitude lower than that of Cu_{Ca}.

Cu_{Ca}, as we now show, contributes to the dielectric response of single-crystal CCTO. We first analyze the structure of both defects, depicted in detail in Fig. 2. We then discuss the dipole, reorientation energetics, and screening properties of Cu_{Ca}. The Ca_{Cu} antisite maintains a configuration similar to the undefected (Cu-occupied) site. Coordination is largely imposed by the TiO_6 tilting pattern, and an isolated Ca insertion is not able to disrupt it. Ca-O bonds are somewhat, though not dramatically, longer than Cu-O bonds (2.2 Å vs 2.0 Å). The Ca_{Cu} antisite, a 2+ ion in an [Ar] configuration,

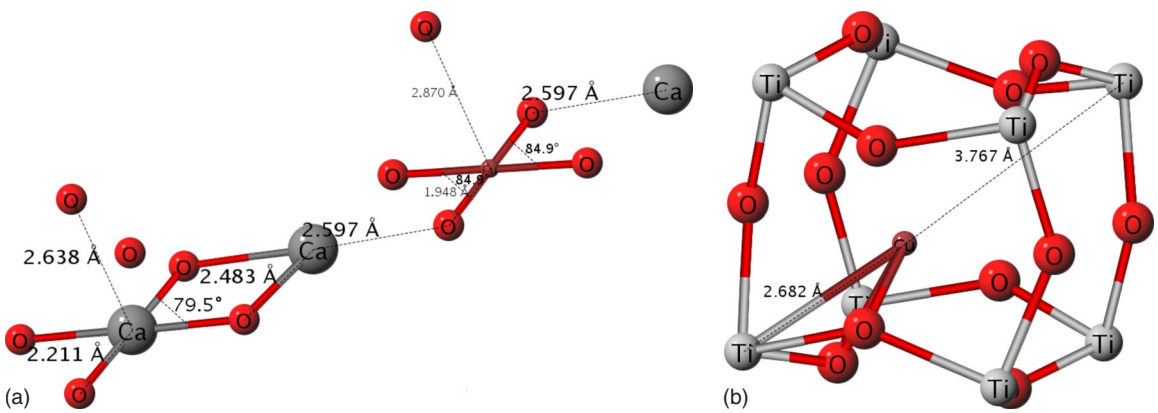

FIG. 2. (Color online) Left panel: Ca_{Cu} antisite. The Ca antisite stretches the distances with the first O shell and brings closer the second shell. Right panel: Cu_{Ca} antisite. The defect moves off-center along the cube diagonal, and its fully relaxed position lies slightly outside the diagonal direction.

TABLE I. Transition barriers for Cu_{Ca} reorientation. The diagonal path through the cube center is most favored.

	Transition points	End points	Barrier (eV)
Cube diagonal	1	7	0.11
Face diagonal	3	3	0.18
Corner	3	1	0.27

modifies very slightly the electronic structure, and in particular inserts no state in the transport gap of CCTO. The Cu-localized d^9 hole is now absent, with an attendant local decrease in magnetization.

The Cu_{Ca} antisite, on the other hand, exhibits significant relaxations. While the Ca site is at the center of the cube with vertexes on the neighboring Ti ions, the Ca-substituting Cu departs from the cube center and moves toward one of the Ti vertices. Cu_{Ca} has thus eight equivalent distortion directions—each being actually threefold, as Cu goes slightly off the cube diagonal toward one of the three neighboring oxygens. Each of these configurations carries a dipole. The ionic-charge times displacement estimate of ~ 1.1 eÅ is confirmed by the direct calculation of the polarization difference upon distortion via the Berry-phase approach,[18] giving $|\Delta \mathbf{P}| = 1.3$ eÅ$= 6$ D (for comparison, the largest diatomic-molecule dipole is 10 D). Cu_{Ca} has a half-filled weakly spin-polarized level in the antiferromagnetic gap. Such residual quasidegeneracy is most probably a GGA artifact. Indeed, GGA+U restores a 0.1 eV gap between an occupied majority and an unoccupied minority states.[19] (The Berry-phase calculation was done with GGA+U, which describes the defected system as insulating.)

The reorientation of the large dipole of Cu_{Ca} involves the displacement of the Cu ion between adjacent minima about 1 Å apart along the cube diagonal. The energy barriers between different defect orientations will determine how easily the dipole reorients. We studied the total energy of intermediate configurations[20] along three kinds of high-symmetry paths: one through the cube center, which enables seven different reorientations; another through the cube face center, allowing for nine paths and six inequivalent reorientations; the last through the corner center, which allows for three different reorientations. Results for the different paths are summarized in Table I. The path through the cube center is favored, with a 0.11 eV activation energy; the other paths, however, are also fairly easy for Cu to go through.

It has been known for some time that the lattice dielectric constant of CCTO is large but not anomalous [a local-density approximation (LDA) calculation[10] gave about 50; our own GGA calculation for the similar compound $CaZn_3Ti_4O_{12}$ gives about 90] and is dominated by IR-active modes mostly consisting of Ca oscillations around the cubic A site. To check for possible anomalies induced by Cu_{Ca}, we calculated the normal modes of Cu_{Ca} at its equilibrium position near the A site, and of Ca at its own A site, in the otherwise frozen crystal. The three Ca frequencies are 185 cm^{-1}, while those of Cu_{Ca} are between 185 and 145 cm^{-1}. (The latter is the same as that of Ca when rescaled by the mass-ratio factor: the "spring constants" of Cu_{Ca} are therefore stiffer on average.) These results rule out Cu_{Ca}-induced vibrational dielectric anomalies.

Our proposal is that the screening mechanism enacted by Cu_{Ca} is a dipole reorientation upon Cu_{Ca} displacement between equivalent minima. We have shown so far that Cu_{Ca} is an abundant low-symmetry dipole-carrying, easily reorientable defect; as such, it will contribute significantly to dielectric screening. We now examine the consistency of the properties of Cu_{Ca} with the intensity, as well as with the frequency and temperature behavior, of the dielectric response. In the simplest charged oscillator model the dielectric constant is $\varepsilon = 1 + nZ^2/\epsilon_0 m\omega$, with n, m, and Z the density, mass, and ionic charge of Cu_{Ca}, and ω a characteristic frequency to be discussed below. ε is of order 10^8 for the maximum n attainable in Cu-rich conditions. This means that anomalous ε values (say, 10^4) may occur already at concentrations around 10^{15} cm^{-3}, easily reachable even in nonextreme growth conditions. (Of course, the hypothesis of a defect-originating anomalous screening is compatible with the somewhat erratic dielectric constants in different samples and preparation conditions.)

Concerning frequency and temperature dependence, we note that Cu_{Ca} has several equivalent minima so that an external field will drive the Cu ion into another available minimum whenever the ion is thermally excited out of the minimum it sits in. (A purely field-induced transition is unlikely as, from the calculated barrier height and interminima distance, it would require fields of order 1 MV/cm.) From the calculated transition barrier of 0.1 eV, transition-state theory predicts full thermal activation off these minima (arbitrarily defined as a transition rate of 1 Hz) at $T \sim 40$ K (we use as vibrational prefactor the 145 $cm^{-1} = 4.3$ THz vibrational frequency calculated above for Cu_{Ca}). Once the Cu ion is free to move, it will be displaced to an equivalent minimum by the external field, and the dipole will thereby be reoriented. In a static or low-frequency field, the reorientation will be instantaneous compared to the field's time variation, and the response will start up sharply at the activation temperature. This is indeed the case of the dielectric constant measured vs T at 0.1 Hz (Ref. 3, Fig. 1, upper panel), which has a sharp kink at about 50 K. We note also that the other reorientation paths would start to activate around 100–150 K, respectively; the low-frequency dielectric constant does indeed show a second broad knee at about 170 K.

As the frequency is raised, the response will become more and more sluggish. In fact, the dipole reorientation is in fact a bodily motion of the Cu ion from one minimum to another. The transit time of Cu between two minima separated by ℓ under a field E, i.e., between two dipole orientations, is $\sqrt{2\ell m/eE}$ assuming classical motion. For plausible numbers ($\ell = 1$ Å, $E = 50$ V/m) the inverse of this time is of order 50 MHz; this is also the characteristic frequency ω we plugged into our above estimate of ε. The frequency is in order-of-magnitude agreement with the cutoff of the anomalous response at frequencies between 10 and 100 MHz.[3]

Purposely planned experiments would be of the utmost interest to test our proposal. An obvious place to look for a Cu_{Ca}-enhanced dielectric constant are CCTO single crystals (which in principle do not contain internal barrier layers)

grown in Cu-rich conditions (giving abundant Cu_{Ca}). Each Cu_{Ca} carries a small (0.5 μ_B) magnetic moment and should be revealed by neutron scattering, EPR, and weak ferrimagnetic susceptibility—although the concentration is probably too low for reliable detection.

In summary, we presented an *ab initio* study of *A*-cation antisites in CCTO, showing that in typical growth conditions (a) Ca_{Cu} reaches concentrations of 10^{14} cm^{-3}, above which $CaTiO_3$ formation (often observed experimentally) is expected; (b) the Cu_{Ca} antisite can reach concentrations of 10^{19} cm^{-3} in Cu-rich conditions, which can be associated with more controllable O-lean conditions; (c) Cu_{Ca} spontaneously distorts into a multiple-minimum low-symmetry dipole-carrying configuration, which can be easily be reoriented by combined temperature and field. This reorientation entails a large dipole variation. Our estimates of the activation temperature, cut-off frequency, and value of the ensuing dielectric constant fall in the experimental range. We thus propose that the Cu_{Ca} defect may be responsible—or coresponsible—for the anomalies in the low-temperature nonintrinsic dielectric behavior in single-crystal CCTO.

Work supported in part by the European Commission via Projects NUOTO, ATHENA, OxIDes; by MIUR via the project Cybersar; and by a Fondazione Banco di Sardegna 2008 grant. Computing resources at CASPUR Rome were provided under a SLACS-CASPUR agreement, as well as by CASPUR supercomputing grants.

[1] C. C. Homes, T. Vogt, S. M. Shapiro, S. Wakimoto, and A. P. Ramirez, Science **293**, 673 (2001).

[2] P. Lunkenheimer, V. Bobnar, A. V. Pronin, A. I. Ritus, A. A. Volkov, and A. Loidl, Phys. Rev. B **66**, 052105 (2002).

[3] P. Lunkenheimer, R. Fichtl, S. G. Ebbinghaus, and A. Loidl, Phys. Rev. B **70**, 172102 (2004).

[4] M. Cohen, J. B. Neaton, L. He, and D. Vanderbilt, J. Appl. Phys. **94**, 3299 (2003).

[5] M. Maglione and M. A. Subramanian, Appl. Phys. Lett. **93**, 032902 (2008).

[6] T. B. Adams, D. C. Sinclair, and A. R. West, Phys. Rev. B **73**, 094124 (2006).

[7] S.-Y. Chung, I.-D. Kim, and S.-J. Kang, Nature Mater. **3**, 774 (2004).

[8] Unpublished calculations. A preliminary account was given in P. Alippi, V. Fiorentini, and A. Filippetti, ECS Trans. **3**, 291 (2006).

[9] Ch. Kant, T. Rudolf, F. Mayr, S. Krohns, P. Lunkenheimer, S. G. Ebbinghaus, and A. Loidl, Phys. Rev. B **77**, 045131 (2008).

[10] L. He, J. B. Neaton, M. H. Cohen, D. Vanderbilt, and C. C. Homes, Phys. Rev. B **65**, 214112 (2002).

[11] J. P. Perdew, J. A. Chevary, S. H. Vosko, K. A. Jackson, M. R. Pederson, D. J. Singh, and C. Fiolhais, Phys. Rev. B **46**, 6671 (1992).

[12] G. Kresse and J. Furthmüller, Comput. Mater. Sci. **6**, 15 (1996); Phys. Rev. B **54**, 11169 (1996).

[13] P. E. Blöchl, Phys. Rev. B **50**, 17953 (1994); G. Kresse and D. Joubert, *ibid.* **59**, 1758 (1999).

[14] The cell volume is kept fixed in all defect calculations since the formation energy of a diluted defect is calculated at the equilibrium volume of the perfect crystal. See M. Finnis, *Interatomic Forces in Condensed Matter* (Oxford UP, Oxford, 2004), pp. 156–157.

[15] The "simple cubic" or "fcc" labels refer to the lattice occupied by the Ca atoms, which can be assumed as origin of the cell.

[16] G. Makov and M. C. Payne, Phys. Rev. B **51**, 4014 (1995).

[17] P. Fiorenza, R. Lo Nigro, V. Raineri, R. G. Toro, and M. R. Catalano, J. Appl. Phys. **102**, 116103 (2007).

[18] R. D. King-Smith and D. Vanderbilt, Phys. Rev. B **47**, 1651 (1993); R. Resta, Rev. Mod. Phys. **66**, 899 (1994). The **k**-space integration for the Berry phase of the defected system was done on a $2\times2\times6$ Monkhorst-Pack mesh and cyclic permutations.

[19] We use the Dudarev formulation [S. L. Dudarev, G. A. Botton, S. Y. Savrasov, C. J. Humphreys, and A. P. Sutton, Phys. Rev. B **57**, 1505 (1998)] implemented in VASP. The free parameter $U-J=4$ eV on Cu *d* states is chosen to reproduce the self-interaction-corrected gap (Ref. 8).

[20] Nudged-elastic-band calculations tended to disrupt antiferromagnetic order and were not pursued further.